

Web Accessibility Statement: If you find any part of this document to be inaccessible with assistive technology, visit our Accessibility web page at conservation.ca.gov to report the issue and request alternative means of access. To help us respond to your concern, please include the following three items in your request: 1. your contact information. 2. the title of this document. 3. the web address where you obtained the document.

CALIFORNIA GEOLOGICAL SURVEY
FAULT EVALUATION REPORT FER-271

Main Strand of the SAN CAYETANO FAULT
in the Fillmore Quadrangle
Ventura County
California

by
Brian P.E. Olson
February 18, 2021

INTRODUCTION

The San Cayetano Fault (SCF) is a major east-west-trending, north-dipping reverse fault, which partially bounds the northern edge of the Santa Clara River Valley along the base of the Topatopa Mountains (Figures 1 and 2). The mapped strands of the San Cayetano Fault are mainly in the foothills along the southern flank of the mountains and in the alluvium near the base of the hills (Weber *et al.*, 1973; Çemen, 1977; Rockwell, 1983; Dibblee, 1991; and Yerkes and Campbell, 1995). The overall fault system (Figure 1) extends from Upper Ojai Valley eastward to Fillmore, and then along the base of the mountains where total separation on the fault diminishes and ultimately dies out in the subsurface approximately 5 km east of Piru (Çemen, 1977). The fault is divided into two sections based on a prominent right-step in the fault trace forming a lateral ramp at Sespe Creek near the town of Fillmore, west of the study area (Rockwell, 1988). The eastern segment is located east of Sespe Creek along the southern margin of the Modelo Lobe and the western segment is mapped high up within the bedrock hills west of Sespe Creek (Çemen, 1977; Huftile and Yeats, 1995; Yerkes and Campbell, 1995). In the current study area, the eastern segment of the SCF consists of a single fault trace at the base of the mountain front, herein referred to as the main strand. A secondary splay, named the "Goodenough Strand" by Çemen (1977), is mapped within the southwestern Modelo Lobe foothills (Plate 1).

Portions of the SCF were previously evaluated by the California Geological Survey and zones of required investigation established around fault strands of the SCF that met the criteria of "sufficiently active" (surface displacement during Holocene time) and "well-defined" (Bryant and Hart, 2007). Kahle (1985 and 1986) evaluated the SCF and established a zone of required investigation from Sespe Creek in the Fillmore Quadrangle west to upper Ojai Valley. More recently, Olson (2012a, b) evaluated and zoned portions of the SCF in the Piru Quadrangle to the east. The evaluation of Olson (2012a, b) was restricted to the Piru Quadrangle, leaving an ~8-km-long gap in zoned faults between Sespe Creek and the eastern boundary of the Fillmore Quadrangle. This study uses available geologic mapping, site-specific fault investigations, combined with an analysis of lidar and aerial imagery to evaluate the Main Strand, Goodenough, and southern San Cayetano strands of the San Cayetano Fault within this gap for surface rupture hazard. Those faults determined in this evaluation to meet the criteria of "sufficiently active" and "well-defined" are recommended to be zoned by the State Geologist as directed by the Alquist-Priolo Earthquake Fault Zoning Act.

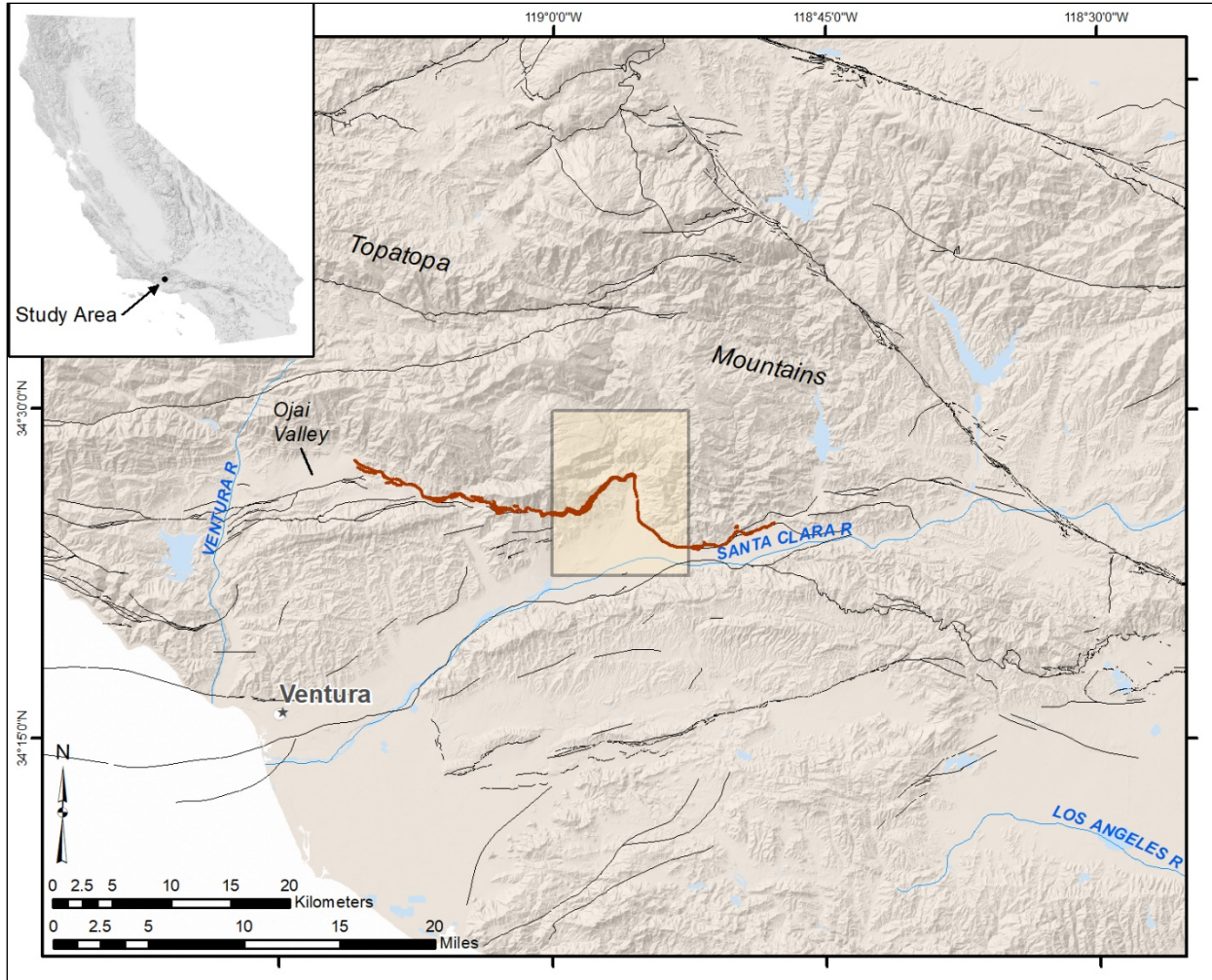


Figure 1. Study area index map showing Fillmore quadrangle (shaded rectangle). Thick red line is the San Cayetano fault. Blue lines are major rivers, black lines are Quaternary active faults.

SUMMARY OF AVAILABLE DATA

The Fillmore study area is located in the southwest portion of the Transverse Ranges geomorphic province. In this area, deformation is dominated by roughly east-west trending low-angle reverse faulting and folding driven by north-south tectonic compression (Shaw and Suppe, 1994).

East of Sespe Creek the SCF runs at the southern base of the Modelo Lobe, which is dominated by the Miocene Modelo Formation, but also includes strata ranging from the Eocene Matilija Sandstone to the Miocene Rincon Shale, which are all faulted and folded into a series of anticlines and synclines whose fold axes generally trend east-west (Weber *et al.*, 1973; Çemen, 1977; Dibblee, 1990; Hufnagle and Yeats, 1995; Yerkes and Campbell, 1995). West

of Sespe Creek the SCF is located higher up the slope, just south of the ridgeline. Bedrock north of the fault zone consists of the same units as to the east; however, south of the SCF the Pliocene Pico Formation and Plio-Pleistocene Saugus Formation are exposed in the low foothills. The Saugus Formation is informally divided into two members: a lower marine member composed of

conglomerate, silty sandstone with minor siltstone beds and a non-marine upper member consisting of chiefly massive sandstone and pebble conglomerate. Late Quaternary alluvium is mapped in the Sespe Creek and Santa Clara River alluvial valleys and as coalescing alluvial fans emanating from the various canyons in the mountains north of the Santa Clara River Valley (Weber *et al.*, 1973; Çemen, 1977; Dibblee, 1990; Yerkes and Campbell, 1995).

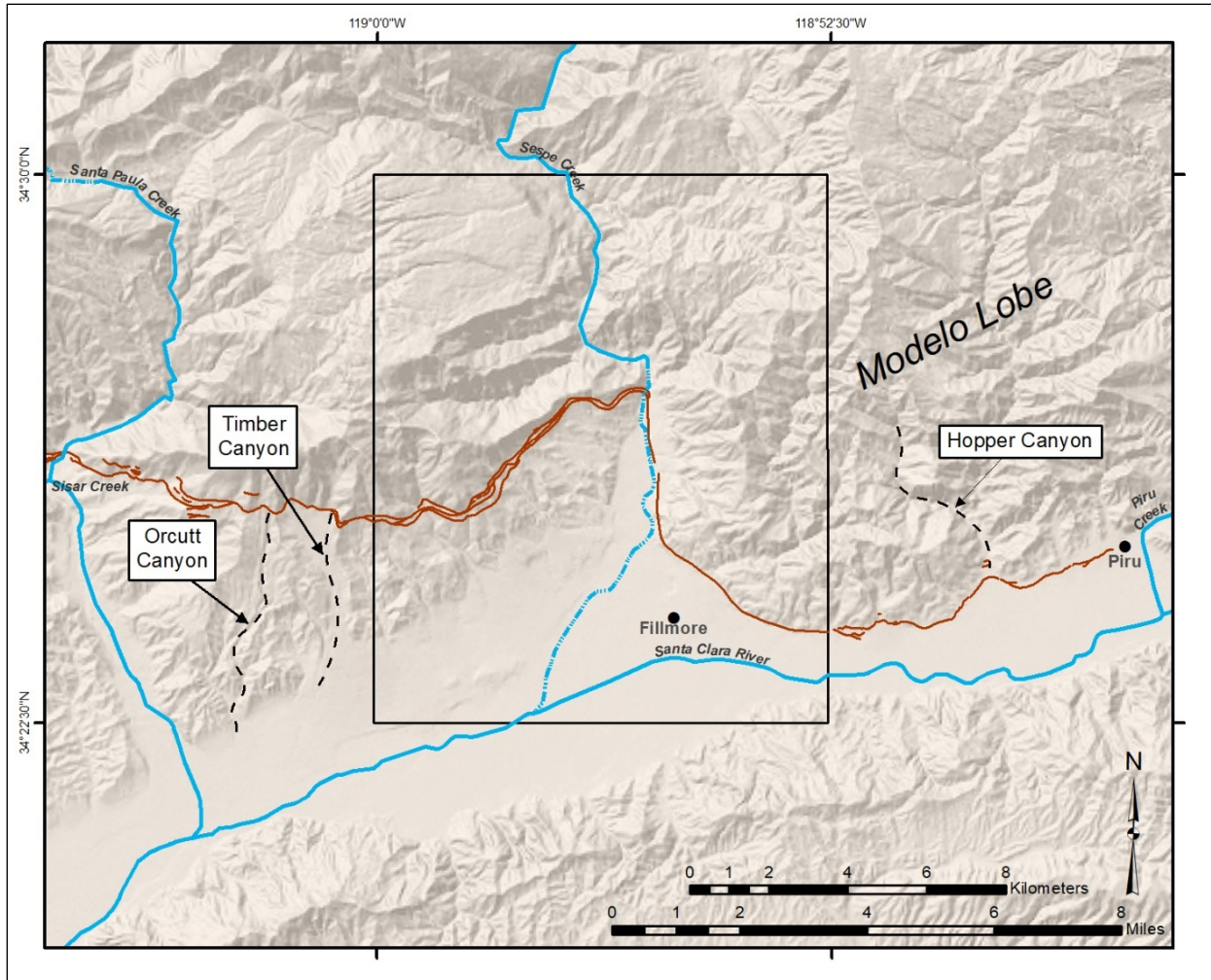


Figure 2. Study area index map showing Fillmore quadrangle boundaries and geographic locations and features referenced in the text. Red lines are surface traces of the San Cayetano Fault Zone.

Topography in the study area is generally mountainous to the north, with the relatively flat Sespe Creek and Santa Clara River valleys draining south and east across the southern part of the quadrangle. All drainages within the Topatopa Mountains in the study area ultimately flow into either of these bodies of water.

LITERATURE REVIEW

The San Cayetano Fault is characterized as a thrust fault due to the relatively low dip angles and reverse separation of stratigraphic units. Based on geologic mapping and well data, the fault plane

dips at a very low angle in the shallow subsurface and becomes gradually steeper with depth (Çemen, 1977, 1989; Yeats, 1983; Yeats *et al.*, 1994; Nicholson *et al.*, 2007; Levy *et al.*, 2019). Measured and inferred dips for the near-surface portion of the fault range from as little as 5° to 10° (Yeats, 1983; Çemen, 1989; URS, 2014) up to 20° to 60° (URS, 2014). Çemen (1989) indicates both the Main and Goodenough strands merge at depth into a single fault plane that gradually increases in dip up to 45°.

Cumulative dip-slip displacement on the San Cayetano Fault has proven difficult to determine because the oldest units in the hanging wall have yet to be encountered in any wells drilled to date in the footwall of the fault (Çemen, 1977 and 1989). Rockwell (1988) and Çemen (1989) both calculate approximately 7,500 meters of total stratigraphic separation on the Modelo Lobe segment of the fault using the maximum thickness of the bedrock units in both the hanging wall and footwall. Separation decreases notably to the east on both strands, such that the Main Strand dies out under Piru Canyon, approximately 12 km to the east of the study area.

Quaternary slip rates for the Modelo lobe portion range from 7.3 to 7.5 mm/yr (Rockwell, 1988; Çemen, 1989; Huftile and Yeats, 1996), which is significantly higher than rates calculated for the portion west of Sespe Creek of approximately 1 to 3.6 mm/yr (Rockwell, 1988). Dolan and Rockwell (2001) note the slip rate for the segment east of Sespe Creek is one of the highest for any reverse fault known in California.

Workers who have mapped this portion of the San Cayetano Fault include: Weber *et al.* (1973), Weber *et al.* (1975), Çemen (1977 and 1989), Rockwell (1983 and 1988), Dibblee (1990), Yerkes and Campbell (1995), and Tan (1998). Several trenches were also excavated and logged across the Main Strand by URS (2014). Other researchers who have worked on regional tectonics studies involving the San Cayetano Fault characteristics are Yeats (1983), Huftile (1993), Huftile and Yeats (1996), Nicholson *et al.* (2007), Hubbard *et al.* (2014), Hughes *et al.* (2018), and Levy *et al.* (2019). The surface traces of the San Cayetano Fault Zone mapped by various workers are depicted on Plate 1.

Previous CGS Fault Evaluation Reports

The San Cayetano Fault system was previously evaluated under the guidelines of the Alquist-Priolo Earthquake Fault Zoning Act (Bryant and Hart, 2007) in 1977, 1985, and 2012. For the initial fault evaluation, Smith (1977) reviewed the fault in its entirety from Ojai to Piru. In the current study area, he relied mainly on mapping by Weber *et al.* (1973 and 1975) who only mapped the principal strand of the fault buried along the base of the mountains thrusting bedrock over Quaternary alluvium (Plate 1). North of Fillmore, the fault is mapped diagonally crossing the Sespe Creek alluvial plain to connect with a bedrock fault in the foothills. The northernmost strand of the SCF is shown crossing the mouth of Sespe Canyon and turning south for about 1,500 m in the canyon alluvium before turning southeast and trending into the foothills where it loses separation and dies out. Zoning was not recommended by Smith for any portion of the San Cayetano Fault because "[w]hile Holocene activity has been suggested, it has not been proven."

Using newer data, which included geologic mapping by Çemen (1977) and Rockwell (1983), Kahle (1985 and 1986) re-evaluated the San Cayetano Fault and established an Alquist-Priolo Earthquake Fault Zone for the Main Strand of the San Cayetano Fault from Upper Ojai Canyon to Sespe Creek, north of Fillmore.

Most recently, Olson (2012) focused on the SCF in the Piru Quadrangle immediately to the east. That evaluation utilized additional mapping and subsurface data resources not incorporated in previous FERs. Most importantly, paleoseismic trench studies by Dolan and Rockwell (2001) and Dolan (2009) shed light on the existence and activity of the Piru Strand in the alluvial fan sediments outboard of the mountain front. The second new resource was a lidar digital elevation model (Earthscope, 2008) covering the foothills and alluvial fans north of the Santa Clara River. Olson determined the Main Strand west of Hopper Canyon and the Piru Strand met the zoning criteria and included them within an Alquist-Priolo Earthquake Fault Zone extending from the town of Piru west to the Fillmore Quadrangle boundary.

Çemen (1977)

Çemen (1977) mapped traces of the SCF in the Sespe-Piru Creek area from the Fillmore area to approximately 7 km east of Piru, including both strands within the Fillmore Quadrangle (Plate 1), which generally follow mapping by Weber *et al.* (1973 and 1975). Where the Main Strand is mapped in the alluvium near Fillmore and along Sespe Creek, it is delineated based on bedrock exposures, low scarps, and differences in soil color visible in aerial photographs. The Main Strand offsets Tertiary bedrock in the foothills west of Sespe Creek but is depicted as buried under the young alluvium of the creek to the east and along the base of the mountains north and east of Fillmore. Çemen also maps the Goodenough Strand of the SCFZ in the foothills east of Sespe Canyon where it places Lower Miocene Rincon Formation and Upper Oligocene Vaqueros Formation over Middle Miocene Modleo Formation. However, his mapping shows the Goodenough Strand quickly dies out to the east (Plate 1). Çemen also maps a discontinuous thrust he names the Pagenkopp Fault, which trends north-south and terminates perpendicularly into the Main Strand west of Sespe Creek.

Using oil well data, Çemen measured approximately 5,200 to 7,300 m of stratigraphic separation on the Main strand of the San Cayetano Fault about 1.5 km west of Hopper Canyon using "the minimum and maximum thicknesses of the rock units stratigraphically between the lower sandstone member of the Modelo Formation and the base of the Saugus Formation." Separation steadily decreases on both strands to the east such that approximately 1.5 km east of Piru, separation on the Piru strand is about 1,400 m using the same stratigraphic correlation (Çemen, 1989). Approximately 1 km east of the Piru Quadrangle boundary, vertical separation is only 750 m and the Piru Strand loses separation completely and dies out into the Santa Clara Valley syncline 1.3 km farther east. Çemen notes older alluvial fan deposits were mapped as offset by the fault within the study area and concluded the San Cayetano Fault should be considered potentially active.

Çemen (1989)

Çemen (1989) later published a paper on the near-surface expression of the SCF from Sespe Canyon eastward based mainly on data gathered from his earlier thesis, new regional groundwater data, and subsequent studies by others including Rockwell (1983 and 1988). Here, Çemen postulates the cause of the color changes in the soil used to map the near-surface trace of the fault are related to changes in groundwater levels, possibly due to the fault acting as a groundwater barrier in the young alluvium. Based on this data, he ultimately concludes the low scarp and soil color change in the Sespe Creek terrace deposits may suggest the pre-deposition topography was influenced by the SCF.

Dibblee (1991)

Dibblee mapped traces of the San Cayetano Fault as part of his geologic map of the Fillmore Quadrangle. This mapping was originally performed by Dibblee at various times between 1946 and 1990. He mapped the San Cayetano as a single, continuous concealed fault along the base of the mountains from the eastern quadrangle boundary turning north at Sespe Creek where it is mapped immediately west of a series of bedrock cliff outcrops on the edge of the alluvial canyon (Plate 1). From here the fault trends north up to the mouth of Sespe Canyon. West of the mouth of Sespe Canyon he shows the SCF bifurcating into two subparallel fault strands trending west, then southwest, just below the ridgeline. The higher fault appears to form the boundary of a large landslide complex, while the lower strand is concealed below the slide deposits. Like previous mappers, Dibblee does not show any SCF strands offsetting Quaternary alluvial sediments.

Nicholson *et al.* (2007)

Noting the SCF thrusts Neogene bedrock over younger unconsolidated sediments, Nicholson *et al.* (2007) explored the way non-elastic deformational processes in the footwall may contribute to the high rates of crustal shortening measured in the Ventura Basin (Donnellan *et al.*, 1993; Huftile and Yeats, 1996). The authors note the SCF and other basin-bounding reverse faults in this area have rotated nonplanar three-dimensional geometries based on structural cross sections. To explain this, they suggest differential compaction and subsidence of the unconsolidated footwall sediments, induced by the overlying Miocene to Pliocene bedrock units, is causing collapse and rotation of the near-surface portion of the San Cayetano fault plane toward the basin. This differential compaction, subsidence, and fault plane rotation can also generate apparent vertical offset via flexural slip. This non-seismic fault slip may explain the high slip rate calculated for the San Cayetano Fault, especially in the Modelo Lobe region.

As a result of the footwall compaction and subsidence, coupled with on-going hanging wall uplift and basinward tilting, Nicholson *et al.* (2007) also suggest there is an increased potential for gravity sliding toward the basin, which can add to the nonplanar fault plane geometry and total vertical offset. They postulate this is the case with the Modelo Lobe portion of the San Cayetano Fault (Figure 2). Here they state the three-dimensional geometry of the fault plane, derived from structure contour maps and detailed cross sections, is reminiscent of a thrust nappe. Their postulated model proposes the Modelo Lobe formed as a "deep-seated, gravity-driven failure" and the near-surface displacements on the shallow-dipping Modelo Lobe portion of the San Cayetano Fault are caused by both fault slip at depth and sliding of the uplifted bedrock in the hanging wall. The authors claim this "mega-slide" most likely failed within the Rincon Formation, which is a weak shale bedrock unit prone to bedding plane and detachment slip and underlies the Modelo Formation.

The authors conclude if their proposed footwall subsidence/compaction and gravity-induced sliding model is correct, it has significant implications for fault modeling and concomitant seismic hazard analysis. They summarize that non-elastic deformation, mainly in the form of compaction, subsidence, and gravity sliding, may be accommodating regional tectonic strain in the Ventura Basin. Also, in this model, compaction of the young sediments in the footwall alone can produce fault plane deformation, increased vertical separation, and horizontal motion mimicking co-seismic fault slip. Therefore, Nicholson *et al.* conclude these effects would contribute to the horizontal and vertical motions seen in the geologic data and measured in geodetic surveys,

which could result in an overestimation of the inferred seismic hazard for these basin-bounding faults.

URS (2014)

URS conducted a fault investigation in 2014 as part of their overall geotechnical study of the Fillmore Works site, a former oil refinery and crude oil pumping facility east of Fillmore at the base of the mountains (Locality 1 on Plate 1). A total of 10 trenches were excavated to locate the surface trace of the SCF (Figure 3). They began with two fault trenches (Trenches 1 and 2) excavated across a distinct geomorphic scarp. The trenches ranged from 90 to 95 feet long and were on the order of 10 feet deep. They exposed the SCF, which thrust Modelo Formation bedrock over Holocene alluvium in both trenches. Trench 1 encountered the fault in the extreme northeastern end where it dipped 20° northeast at the bottom of the trench and steepened to 60° at the surface (Figure 4a). Much more of the fault was observed in Trench 2 where pervasively sheared Modelo bedrock was thrust over alluvium. The fault enters the bottom of the trench dipping 6° east, flattens to nearly horizontal, and steepens to about 36° as it emerges to the surface. Subsequent to these initial trenches, URS excavated an additional seven fault trenches at the site. URS geologists observed individual strands of the SCF in Trenches 7 through 9, even though there were logged from the surface only due to trench safety concerns (Figures 4b and 5). Each of these trenches exposed the fault wholly within the alluvium. Additionally, the consultants logged an open storm drain trench excavated at the site across the trace of the SCF. This trench exposed the fault where it thrust alluvium over colluvium. Lastly, the URS consultants drilled 16 hollow-stem auger borings along a linear transect perpendicular to the fault. Based on stratigraphic anomalies within the alluvium, URS identified active traces of the SCF at the eastern end of the transect.

URS also inferred an "upper strand" of the San Cayetano Fault zone in the foothills east of the project site based on an exposure of over Modelo Formation bedrock over older alluvium in a railroad right-of-way cut slope (Plate 1). Because this older alluvial deposit is above the Q3 terrace surface it is necessarily older, and the consultants note the older alluvium is most likely late Pleistocene with a maximum age of about 126ka. Therefore, at the latest, this fault initiated in the late Pleistocene, and requires numerous rupture events over that time to bring Miocene bedrock up and over older alluvium. URS did not trench this fault in their investigation, and therefore, conclude "[w]hether or not it is Holocene active is unknown."

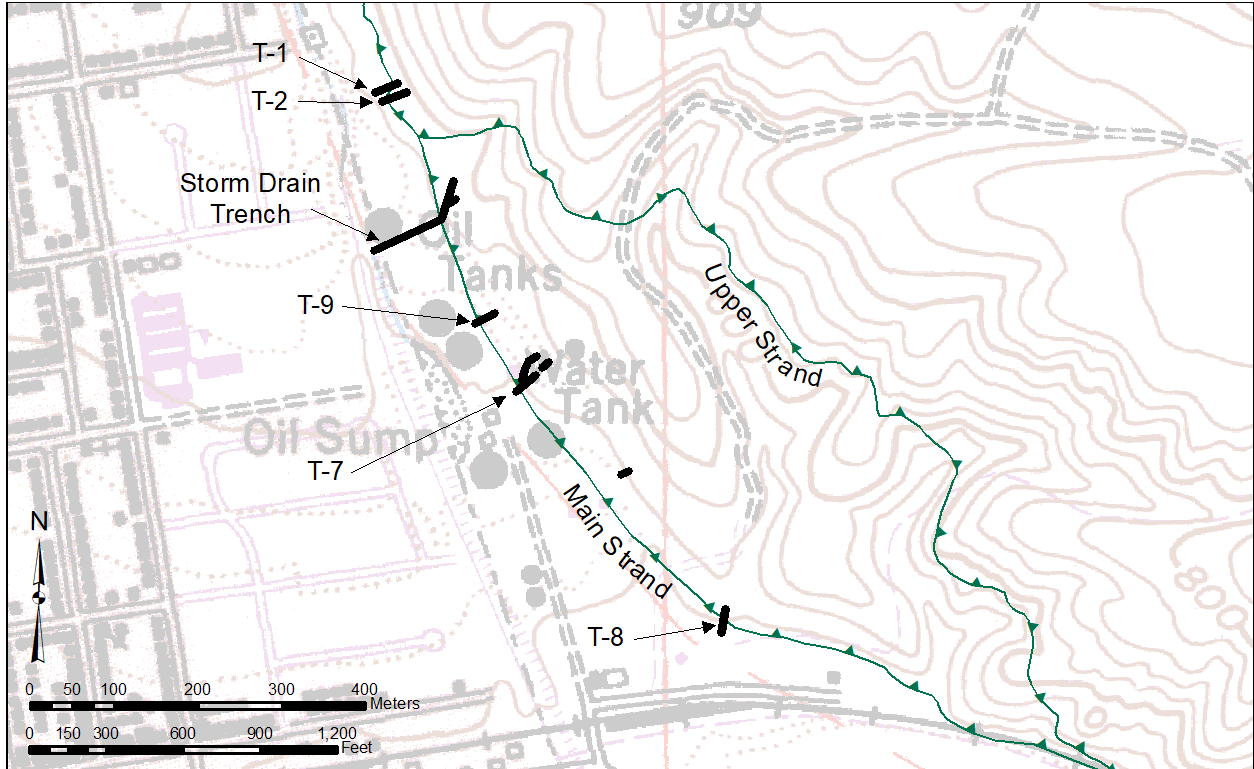


Figure 3. Mapped fault traces and trench locations from the URS (2014) fault investigation. Labeled fault trenches are specifically mentioned in the text.

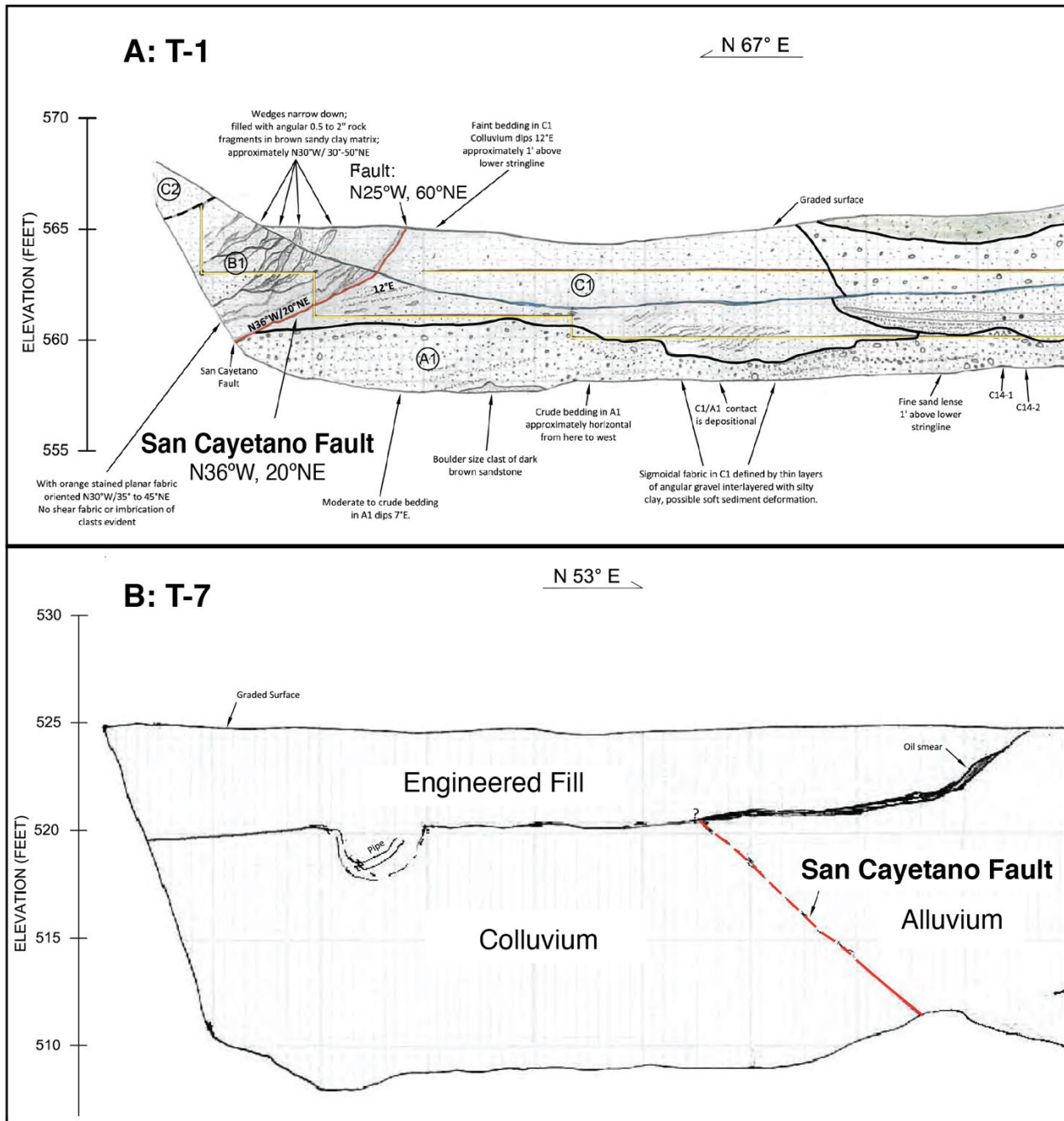


Figure 4. Graphic logs of trenches T-1 and T-7 from the URS (2014) study at the former Fillmore Works site depicting the major geologic units and identified principal fault strands. Vertical scale is elevation, in feet above mean sea level (modified from URS, 2014). See Figure 3 for trench locations

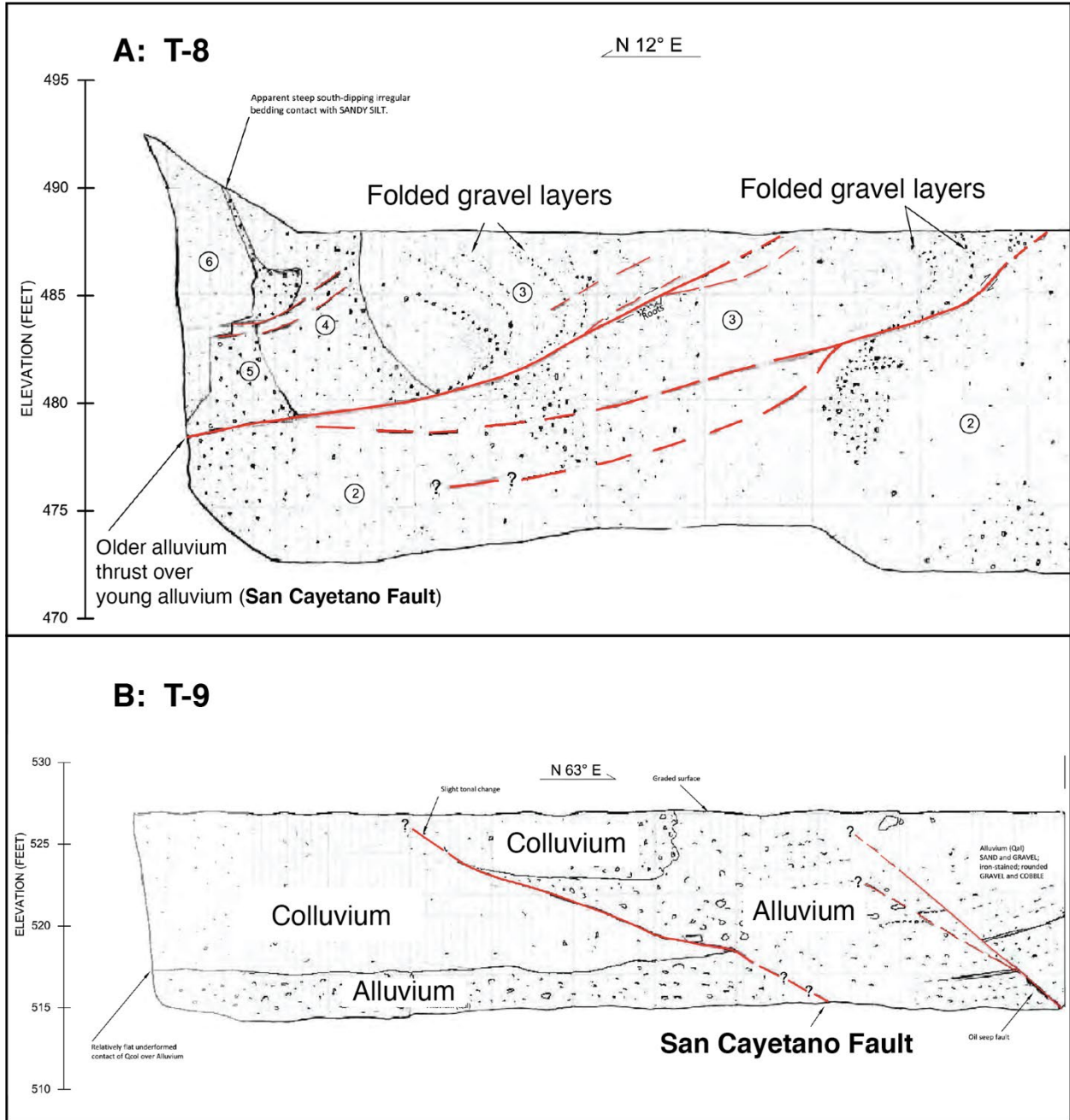


Figure 5. Graphic logs of trenches T-8 and T-9 from the URS (2014) study at the former Fillmore Works site depicting the major geologic units and identified principal fault strands. Vertical scale is elevation, in feet above mean sea level (modified from URS, 2014). See Figure 3 for trench locations.

Hubbard *et al.* (2014) and Hughes *et al.* (2018)

Hubbard *et al.* (2014) developed a regional tectonic model for the Ventura Basin based on well-log and seismic reflection data, which suggested the Ventura Fault merged with the SCF at depth. However, the modeled fault geometries required an additional steeply dipping fault to link them. This fault was referred to as the Southern San Cayetano Fault (SSCF). Hughes *et al.* (2018) subsequently investigated the northern margin of the Santa Clara River Valley for evidence supporting this proposed fault's existence.

Hughes *et al.* (2018) reviewed a digital elevation model (DEM) for the mountain-front area west of Sespe Creek and identified several uplifted and tilted terraces and alluvial fan deposits along the northern edge of the Santa Clara River Valley near the location of the SSCF proposed by the Hubbard *et al.* (2014) model. Specifically, the authors noted alluvial fans crossing the mouth of Orcutt Canyon west of the study area in the Santa Paula Peak Quadrangle (Figure 2) are warped creating south-facing scarps parallel to the mountain front. These deformed surfaces correlate to Q4 and Q5 units mapped by Rockwell (1988) and were dated using ^{10}Be cosmogenic age dating at approximately 7 ka and 19 ka, respectively. Clear surface deformation of alluvial fans along the mountain front continues east of Orcutt Canyon to Timber Canyon (Figure 2). From here to Sespe Creek they note there is no clearly observable deformation; however, they documented a folded Q5 surface about 2 km away from the mountain front in the Santa Clara River Valley (Locality 2 on Plate 2) dated at about 17 ka.

Subsurface data suggested the SSCF dips north between 50° and 90° to a depth of about 100 m where it flattens to approximately 20° . The SSCF would then connect with the main SCF at about 3 km depth. Based on their new alluvial surface dates and fault geometry model, Hughes *et al.* conclude the SSCF initiated about 58 ka at the earliest with an average slip rate over that time of 1.3-1.9 mm/year. Uplift rates calculated for the warped surfaces at the mouth of Santa Paula Creek and Orcutt Canyon range from 0.9-1.6 mm/year. Just west of Timber Canyon the uplift rate is noticeably lower at 0.4 mm/year; however, the folded terrace surface at Locality 2 is uplifting at minimum of 1.9 mm/year. As a result, the authors suggest the SSCF is an active near-surface blind fault along the mountain-front from Adams Canyon to Timber Canyon, where it then steps to the south onto a blind *en echelon* splay beneath the Q5 folded surface in the Santa Clara River Valley (Locality 2 on Plate 2; Figure 6).

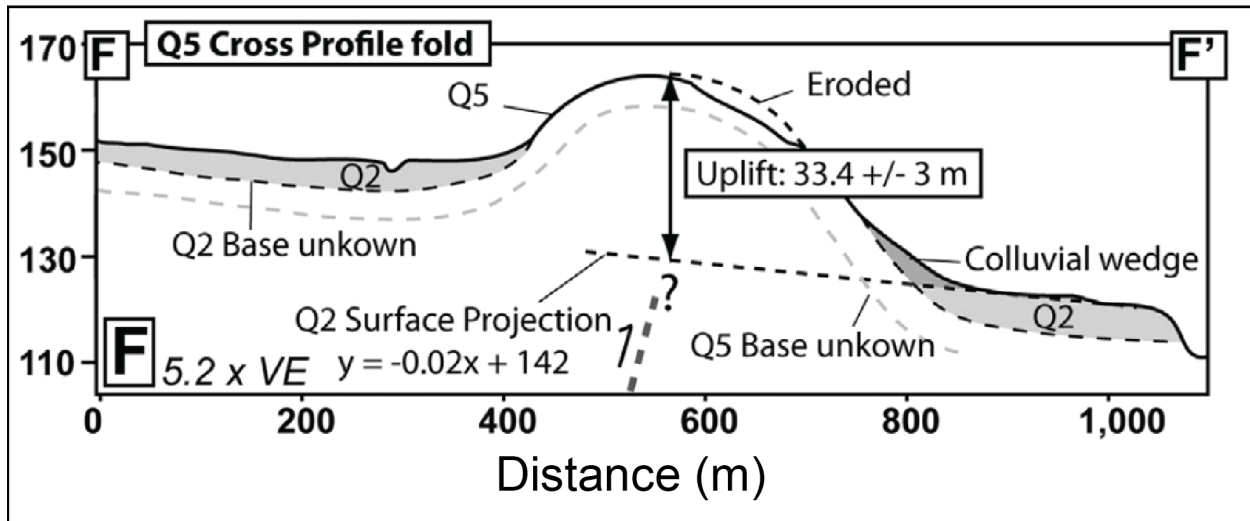


Figure 6. Topographic profile across the uplifted Q5 surface in the Santa Clara River valley (Locality 2 on Plate 2). Solid line is modern topographic surface; heavy dashed line is the postulated low-angle blind thrust fault strand of the Southern San Cayetano Fault zone by Hughes *et al.* (2018); medium dashed line represents the base of the Q2 deposit; light dashed line is the base of the Q5 deposit. See Plate 2 for Q terrace surface ages. (modified from cross section F-F' in Hughes *et al.*, 2018)

Hughes *et al.* (2018) note the SSCF helps explain the noteworthy difference in SCF slip rates calculated west and east of Sespe Canyon. Dolan and Rockwell (2001) determined a slip rate of 7.5 mm/year for the eastern SCF near Piru, but the western SCF slip rate is a maximum of 4.15 mm/year (Rockwell, 1988). Hughes *et al.* (2018) conclude strain in the Ventura Basin, west of Sespe Creek, is partitioned between both the western SCF and the SSCF, with the latter taking up some of the transferred slip from the eastern SCF to the western SCF.

AERIAL PHOTOGRAPHIC INTERPRETATION

Aerial photographic interpretation was performed primarily to look for visual and geomorphic features suggestive of active faulting and also to verify the location and activity of the fault traces mapped by others (Plate 1). This was accomplished using stereo-paired aerial photographs from a flight conducted by NASA in 1994 shortly after the Northridge earthquake. Urban development in the city of Fillmore obscures many portions of the land surface, which makes it difficult to identify geomorphic and tonal features. Even so, some features of the landscape are still evident in areas where development is minimal. Fault traces mapped by others were also checked against these photos for geomorphic evidence of Holocene activity and location accuracy. The various mapped traces and lineaments are annotated and included on Plate 2.

LIGHT DETECTION AND RANGING (LiDAR) DIGITAL ELEVATION MODEL

Two airborne Light Detection and Ranging (LiDAR) surveys of the Santa Clara River Valley were reviewed for this evaluation to more accurately evaluate the geomorphology associated with the San Cayetano Fault in the study area. LiDAR surveys involve scanning the ground surface with a pulsing laser mounted in an airplane. The distance from the laser source to the ground surface is measured based on the time required for the laser beam to be reflected back to the source. Based on the various arrival times a digital model of the ground surface can be generated. The first survey was flown for the County of Ventura Watershed Protection District in February 2005 (Ventura County Watershed Protection District, 2005). The second survey was flown on April 12, 2008 as part of a regional study of southern California fault zones (Earthscope, 2008). For this survey of the Santa Clara River study area, the aircraft flew at an above ground altitude of 700m with a 100 KHz laser pulse frequency resulting in a "point cloud" dataset with approximately 6 to 8 laser point measurements per square meter.

Hillshade relief maps were then derived with 45° and 315° illumination angles at 45° above the horizontal. Additionally, slope aspect-multi-directional hillshade hybrids were derived from the VCWPD dataset. Traces of the San Cayetano Fault identified using the LiDAR-generated hillshade map and contours were plotted directly in ArcGIS.

FIELD INSPECTION

A field visit was made in September 2014 to review some of the open trenches at the former Fillmore Works site (URS, 2014). This visit involved review of the exposed trench walls and a road cut with URS geologists and Dr. Tom Rockwell. A later field visit was performed in January 2020 to check various geomorphic features identified in the aerial photographs and hillshades. Additionally, various slope breaks were observed and recorded using a handheld GPS receiver.

SEISMICITY

Regional seismicity data covering the period from 1981 to 2018 (Hauksson *et al.*, 2012) shows a diffuse pattern of low magnitude earthquake activity over the study area with local areas of swarm activity (Figure 7). The most significant of these was the 2015 Fillmore earthquake swarm (Hauksson *et al.*, 2016). This swarm initiated on July 5, peaked on July 9 and 10, and continued with episodic activity until late September. Over 1,400 earthquakes occurred during this time with the largest earthquake being a M2.8 event on July 9. Cross section A-A' through the swarm shows a strikingly planar seismicity zone dipping 26° north (Figure 8). Based on the hypocentral depths, Hauksson and others infer this fault is a westerly extension of the Simi-Santa Rosa fault. However, it is also possible the swarm source is along the low-angle decollement or blind Ventura fault ramp modeled by Hughes *et al.* (2018). Hauksson *et al.* (2016) state the recorded seismicity suggest this swarm was likely caused by metamorphic dehydration, which released fluids that subsequently migrated and increased fluid pressures along the fault zone.

Overall, there is a notable discrepancy between the magnitude of Holocene offsets measured in fault trenches (URS, 2014; Dolan, 2009; Dolan and Rockwell, 2001) and the noted paucity of significant historical earthquakes in the region. Rockwell (1988) points out clearly "the historic seismicity does not represent the long-term activity."

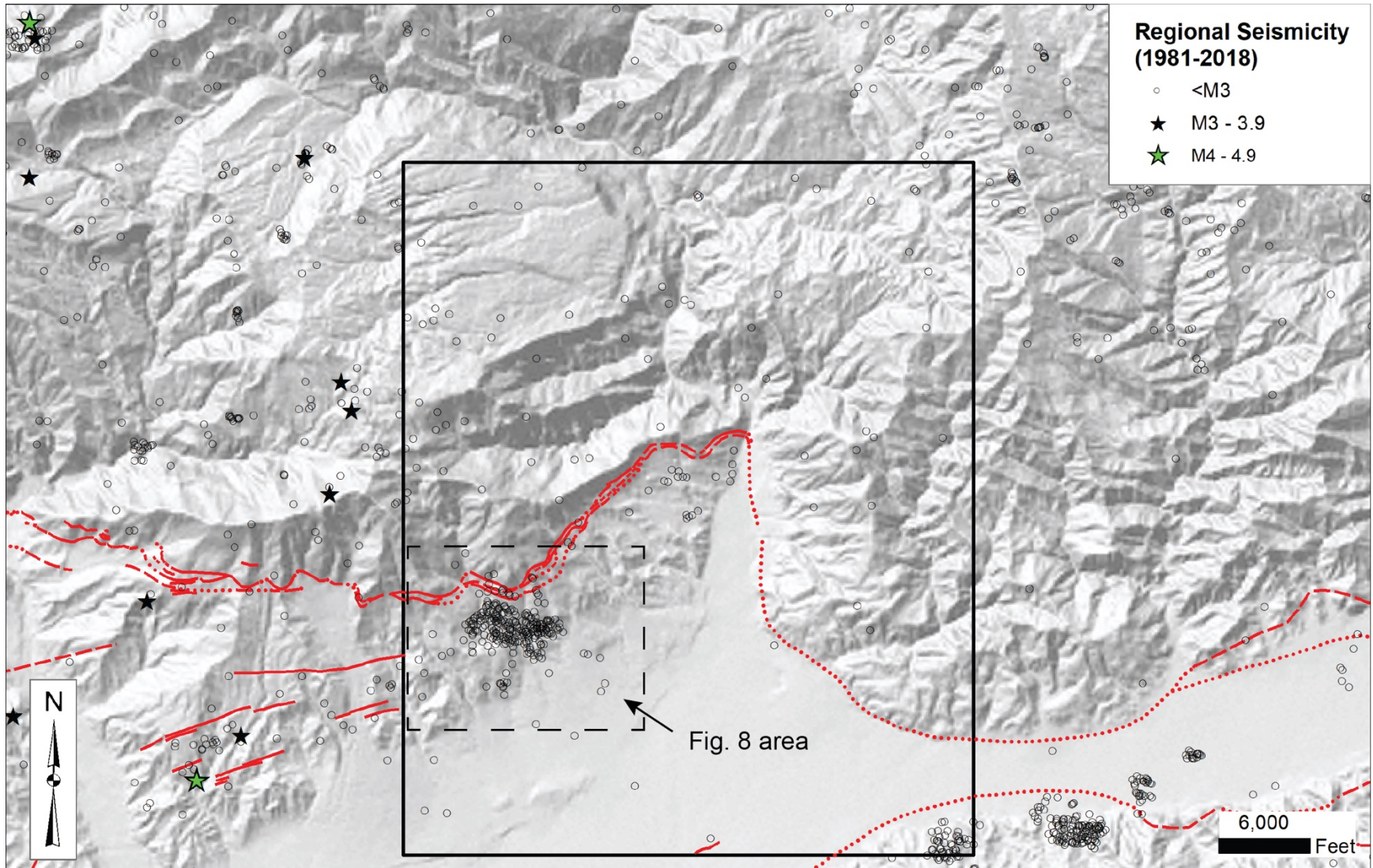


Figure 7. Regional seismicity from 1981-2018 for the Fillmore area. Dashed box highlights epicenters from 2015 earthquake swarm. (epicenter locations from Hauksson et al., 2012)

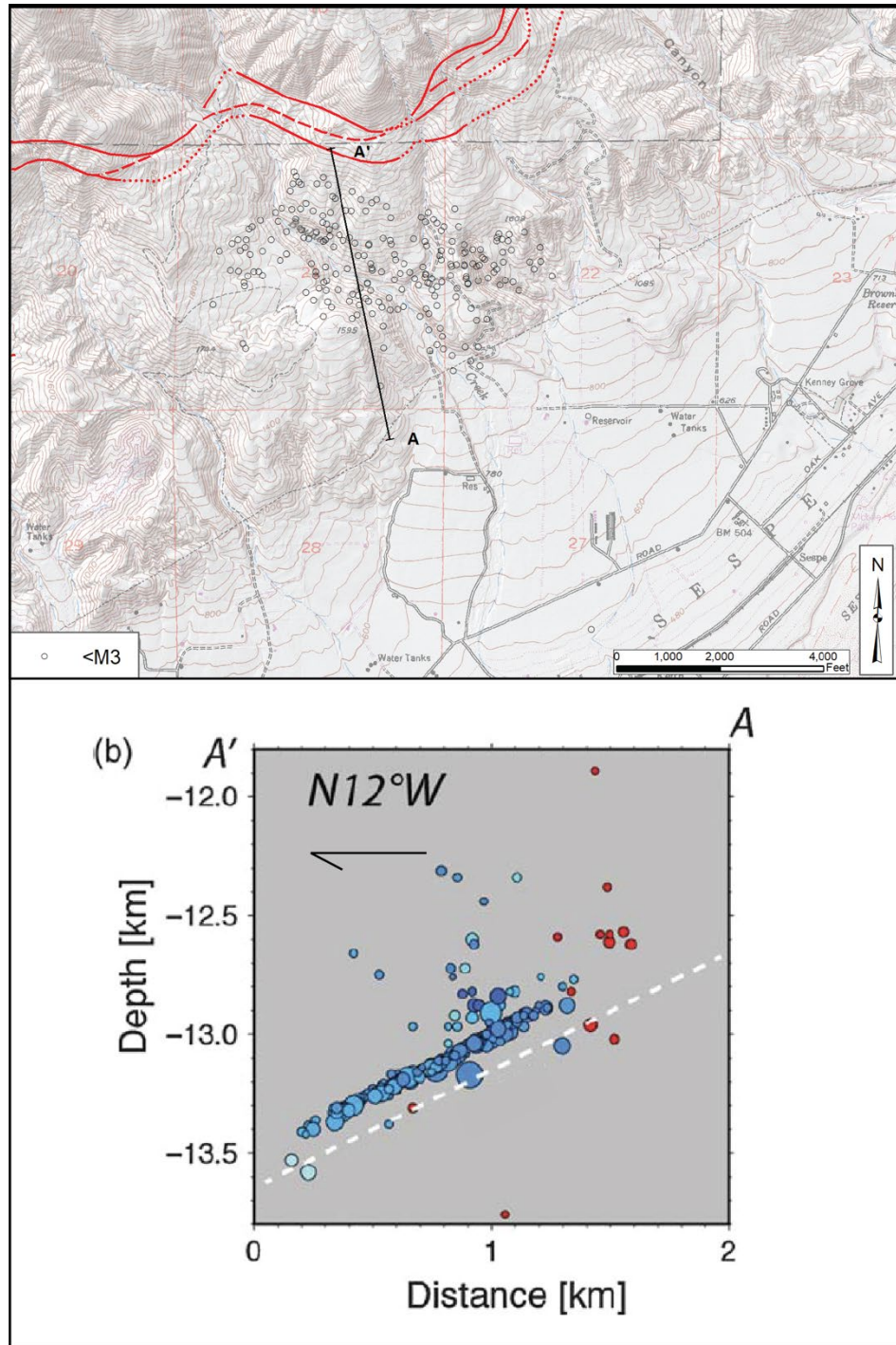


Figure 8. (a) Map of 2015 Fillmore earthquake swarm epicenters. (b) Cross section through the swarm area showing hypocentral depths defining a north-dipping plane. (modified from Hauksson et al., 2016)

DISCUSSION AND CONCLUSIONS

MAIN STRAND

In the Piru Quadrangle immediately east of the current study area, the SCF is moderately well-defined in areas where the fault is located in the alluvium near the base of the mountain front, with several low scarps and breaks in slope (Olson, 2012a, b). However, in the eastern portion of the Fillmore Quadrangle, the mountain front is immediately adjacent to the Santa Clara River, where it is difficult to differentiate potential fault-related scarps from erosional fluvial scarps. Additionally, any previous fault scarps within the Santa Clara River fluvial plain would likely be eroded or masked by deposition, and therefore, not preserved. The fault is presumed to continue west from the Piru area along the base of the mountains. This same problem occurs within the Sespe Creek flood plain north and west of Fillmore.

Northwest of the Santa Clara River channel are several Holocene terrace surfaces associated with the alluvial fans emanating from the adjacent mountains and alluvial process related to Sespe Creek. These terraces were mapped and dated by Rockwell (1988) with additional work by Hughes *et al.* (2018). The former Fillmore Works site (Locality 1 on Plate 2) was developed on the Q3 terrace surface in the early 1900s and was continuously operational into the 2000s. As a result, the original topography was extensively modified to create roads, cut slopes, and tank pads. URS (2014) found the fault in various trenches at this site where it displaced Holocene sediments. Additionally, they identified a secondary reverse fault in the foothills above the site to the east with Miocene bedrock thrust over late Pleistocene alluvium. Given its close proximity to the documented active Main Strand at the mountain front and evidence of multiple events since the late Pleistocene, it is reasonable to conclude this strand could rupture along with the Main Strand.

West of this locality the land surface has been largely modified as the city of Fillmore was developed making it difficult to identify geomorphic features or tonal lineaments on aerial photographs. There is a sharp break in slope immediately west of Pole Canyon and a noticeable scarp above it (Scarp A on Plate 2); however, the slope break is within a residential development that was constructed before 1951. For this reason, it is possible this scarp is modified and not natural.

A short scarp preserved in the Q2 terrace north of Fillmore (Scarp B on Plate 2) may be fault-related. It ranges from 1.5 to 2.5 meters high and is subparallel to the mapped trace of the SCF at this location (Plate 1). Additionally, its location at the base of the mountains is consistent with the SCFZ location east of Sespe Creek to Hopper Canyon (Olson, 2012a,b). However, because of the proximity to the Sespe Creek channel and floodplain, the possibility exists that this is an erosional scarp preserved on the abandoned terrace surface.

Farther north, the steep cliffs along the eastern margin of the Sespe Creek channel expose Tertiary sedimentary bedrock (Plate 2). These outcrops are up to 360 m out from the mountain front and underlie the Q3 terrace surface suggesting this section of the alluvial plain is uplifting along with the mountain block to the east. Consequently, the main surface trace is most certainly west of these outcrops. Any previous geomorphic evidence for surface faulting is either buried or was eroded by Sespe Creek; however, the surface trace is most likely immediately adjacent to the eastern channel margin, paralleling Sespe Creek to connect with the easternmost end of the SCF trace mapped by Kahle (1985) near the mouth of Sespe Canyon (Plate 3). This is generally consistent with previously mapped traces of the SCF (Plate 1).

GOODENOUGH STRAND

The Goodenough Strand is mapped both by Çemen (1977 and 1989) and Weber *et al.* (1973), although in slightly different locations, while Dibblee (1991) does not show any faulting in this area (Plate 1). The aerial photos and lidar hillshades reviewed for this study did not show significant fault-related geomorphology, lineaments, or tonal differences along the mapped locations of the Goodenough Strand suggesting, while this fault strand may exist, it does not appear to have generated surface rupture recently.

SOUTHERN SAN CAYETANO FAULT

Hughes *et al.* (2018) identified the SSCF by mapping and dating deformed alluvial fan surfaces along the mountain front, west of the study area. From Orcutt Canyon and to the east, several of these surfaces are Holocene-age suggesting this fault is active. Calculated uplift rates are reasonably consistent from west to east until Timber Canyon where they drop substantially. This sharp decrease, coupled with the emergent folded surface about 2 km south from the mountain front (Locality 2 on Plate 2), suggests the SSCF steps to the south within the study area. However, because they did not observe any evidence of surface rupture, the authors conclude the fault is blind.

For the current evaluation, stereo-paired photographs, digital satellite imagery, and lidar hillshades were reviewed for evidence of surface faulting along the mapped SSCF. No geomorphic evidence or visible lineaments were observed, which is consistent with the Hughes *et al.* (2018) conclusion.

PAGENKOPP FAULT

Çemen (1977) states the Pagenkopp Fault was first recognized from oil well data, but notes it is not recognized at the surface. His geologic map, however, shows a queried surface fault trace in the foothills west of Sespe Creek (Plate 1). Hughes *et al.* (2018) postulate the Pagenkopp Fault could be an eastward continuation of the SSCF (Figure 2, Plate 1). Based on the low calculated uplift rate at Timber Canyon and the lack of geomorphic scarps to the east, they conclude the Pagenkopp Fault is either not active or blind. This and previous evaluations (Kahle, 1985 and 1986) similarly did not observe any definitive lineaments or geomorphic evidence of surface faulting in this area, which supports this conclusion.

RECOMMENDATIONS

Recommendations for establishing Earthquake Fault Zones are based on the criteria of "sufficiently active" and "well-defined" (Bryant and Hart, 2007).

The principal trace of the **San Cayetano Fault** as shown on Plate 3 is recommended for zoning as it is "well-defined" by trenching studies and mapping, and there is sufficient evidence to conclude it is "sufficiently active" (URS, 2014). The eastern terminus of the previous zone boundary for the SCF established by Kahle (1985) should be modified as depicted on Plate 2 to connect with the newly identified fault trace. While the Southern San Cayetano Fault (Hughes *et al.*, 2018) is demonstrably Holocene active, it is blind within the study area, and therefore does not meet the criterion of "well-defined". No zones are recommended for the Pagenkopp Fault or Goodenough Strand as there is insufficient evidence to demonstrate Holocene activity.



Brian Olson
Engineering Geologist
PG 7923, CEG 2429



Tim Dawson
Senior Engineering Geologist
PG 8502, CEG 2618

REFERENCES

- Bryant, W.A., and Hart, E.W., 2007, Fault-rupture hazard zones in California: California Geological Survey Special Publication 42, 42 p. (digital version only, electronic document available at [Special Publication 42 download](#)).
- California State Water Resources Board (CSWRB), 1956, Ventura County investigation, Bulletin No. 12, two volumes.
- Çemen, I., 1977, Geology of the Sespe-Piru Creek area, Ventura County, California: Ohio University, unpublished M. S. thesis, 69p.
- Çemen, I., 1989, Near-surface expression of the eastern part of the San Cayetano fault: A potentially active thrust fault in the California Transverse Ranges: *Journal of Geophysical Research*, v. 94, p. 9665-9677.
- Dibblee, T.W., Jr., 1990, Geologic map of the Fillmore Quadrangle, Ventura County, California: Dibblee Geological Foundation Map #DF-27, Santa Barbara, California, scale 1:24,000.
- Dolan, J.F., 2009, Paleoseismology and seismic hazards of the San Cayetano Fault Zone: NEHRP Technical Report 02HQGR0041, 20 p.
- Dolan, J.F. and Rockwell, T.K., 2001, Paleoseismologic evidence for a very large ($M_w > 7$), post-AD 1660 surface rupture on the Eastern San Cayetano Fault, Ventura County, California: Was this the elusive source of the damaging 21 December 1812 Earthquake?: *Bulletin of the Seismological Society of America*, v. 91, n. 6, p. 1417- 1432.
- Donnellan, A., Hager, B. H., King, R. W., and Herring, T.A. (1993), Geodetic measurement of deformation in the Ventura Basin region, southern California, *J. Geophys. Res.*, 98, 21,727–21,739.
- Earthscope, 2008, Southern California and Washington (Yakima) fault systems LiDAR survey: National Center for Airborne Laser Mapping (NCALM), flown April 2 through April 26, 2008, 1-meter resolution, http://opentopo.sdsc.edu/metadata/SOCAL_REPORT_final.pdf
- Hauksson, E., Wenzheng, Y., and Shearer, P.M., 2012, Waveform Relocated Earthquake Catalog for Southern California (1981 to June 2011): *Bulletin of the Seismological Society of America*, Vol. 102, No. 5, pp.2239-2244.
- Hauksson, E., Andrews, J., Plesch, A., Shaw, J.H., and Shelly, D.R., 2016, The 2015 Fillmore earthquake swarm and possible crustal deformation mechanisms near the bottom of the eastern Ventura Basin: *Seismological Research Letters*, v. 87, no. 4, p. 807-815.
- Hubbard, J., Shaw, J.H., Dolan, J., Pratt, T.L., McAuliffe, L., and Rockwell, T.K., 2014, Structure and Seismic Hazard of the Ventura Avenue Anticline and Ventura Fault, California: Prospect for Large, Multisegment Ruptures in the Western Transverse Ranges: *Bulletin of the Seismological Society of America*, v. 103, p. 1070-1087.
- Huftile, G.J., 1993, Convergence Rates Across the Ventura Basin, California: Oregon State University, unpublished Ph.D. thesis, 217p.
- Huftile, G. J., and Yeats, R. S., 1996, Deformation rates across the Placerita (Northridge M_w 6.7 aftershock zone) and Hopper Canyon segments of the western Transverse Ranges deformation belt: *Bulletin of the Seismological Society of America*, v. 86, p. S3-S18.
- Hughes, A., Rood, D.H., Whittaker, A.C., Bell, R.E., Rockwell, T.K., Levy, Y., Wilcken, K.M., Corbett, L.B., Bierman, P.R., DeVecchio, D.E., Marshall, S.T., Gurrola, L.D., and Nicholson, C., 2018, Geomorphic evidence for the geometry and slip rate of a young, low-angle thrust

- fault: Implications for hazard assessment and fault interaction in complex tectonic environments: *Earth and Planetary Science Letters*, v. 504, p. 198-210.
- Kahle, J.E., 1985, The San Cayetano Fault and related "flexural-slip" Faults near Ojai and Santa Paula, Ventura County, California: California Division of Mines and Geology Fault Evaluation Report FER-174, (unpublished), 25p., 1:24,000.
- Kahle, J.E., 1986, The San Cayetano Fault near Fillmore, the Lion Fault in Upper Ojai Valley, and the Arroyo Parida-Santa Ana Fault near Mira Monte, Ventura County, California: California Division of Mines and Geology Supplement #1 to Fault Evaluation Report FER-174, (unpublished), 7p., 1:24,000.
- Nicholson, C., Kamerling, M. J., Sorlien, C. C., Hopps, T. E., and Gratier, J.-P., 2007, Subsidence, compaction, and gravity sliding: Implications for 3D geometry, dynamic rupture, and seismic hazard of active basin-bounding faults in southern California: *Bulletin of the Seismological Society of America*, v. 97, p. 1607-1620.
- Olson, B.P.E., 2012a, Eastern San Cayetano Fault in the Piru Quadrangle, Ventura County, California: California Geological Survey Fault Evaluation Report FER-257, (unpublished), 14p., 1:24,000.
- Olson, B.P.E., 2012b, Supplement #1, Eastern San Cayetano Fault in the Piru Quadrangle, Ventura County, California: California Geological Survey Fault Evaluation Report FER-257, (unpublished), 2p., 1:24,000.
- Rockwell, T.K., 1983, Soil chronology, geology, and neotectonics of the north central Ventura Basin, California: University of California, Santa Barbara, unpublished Ph.D. dissertation, 424p.
- Rockwell, T.K., 1988, Neotectonics of the San Cayetano fault, Transverse Ranges, California: *Geological Society of America Bulletin*, v. 100 no. 4, p. 500-513.
- Shaw, J.H. and Suppe, J., 1994, Active faulting and growth folding in the eastern Santa Barbara Channel, California: *Geological Society of America Bulletin*, v. 106, p. 607-626.
- Smith, T.C., 1977, San Cayetano Fault, Ojai, Santa Paula Peak, Fillmore and Piru quadrangles, Ventura County: California Division of Mines and Geology Fault Evaluation Report FER-19, (unpublished), 16p., 1:24,000.
- URS, 2014, Fault rupture and landslide hazard investigation at the Fillmore Works project site, Fillmore, California, report dated October 15, 2014, 5 figures, 7 appendices.
- Ventura County Watershed Protection District, 2005, Lidar data.
- Weber, H.F., Jr., Cleveland, G.B., Kahle, J.E., Kiessling, E.W., Miller, R.V., Mills, M.F., Morton, D.M., and Cilwick, B.A., 1973, Geology and mineral resources study of southern Ventura, County, California: California Division of Mines and Geology, Preliminary Report 14, scale 1:48,000, 5 plates, 102 p.
- Weber, H.F., Jr., Kiessling, E.W., Sprotte, E.C., Johnson, J.A., Sherburne, R.W., and Cleveland, G.B., 1975, Seismic hazards study of Ventura, County, California: California Division of Mines and Geology, Open-File Report 76-5LA, scale 1:48,000, 9 plates, 396 p.
- Yeats, R. S., 1983, Large-Scale Quaternary Detachments in Ventura Basin, Southern California: *Journal of Geophysical Research*, v. 88, no. B1, p. 569-583.
- Yeats, R. S., Huftile, G. J., and Stitt, L. T., 1994, Late Cenozoic tectonics of the east Ventura basin, Transverse Ranges, California: *American Association of Petroleum Geologists Bulletin*, v. 78, p. 1040-1074.

Yerkes, R.F. and Campbell, R.H., 1995, Preliminary geologic map of the Piru 7.5 quadrangle, southern California: U.S. Geological Survey, Open-File Report OF-95- 511, scale 1:24,000.

Yerkes, R.F. and Lee, W.H.K., 1979, Late Quaternary deformation in the Western Traverse Ranges, California: U.S. Geological Survey Circular 799-B, p. 27-37.

AERIAL PHOTOGRAPHS REVIEWED

USGS (US Geological Survey); b/w 9x9; 1:24,000 scale; Flight: EM; Frames 3 – 39; date: 8/16/1947

NASA (National Aeronautics and Space Administration); b/w; 9x9 1:16,250 scale (approx.); Flight: 04689; Frames: 526-534, 614-621; date: 1/22/1994

119°0'0"W 118°58'30"W 118°57'0"W 118°55'30"W 118°54'0"W

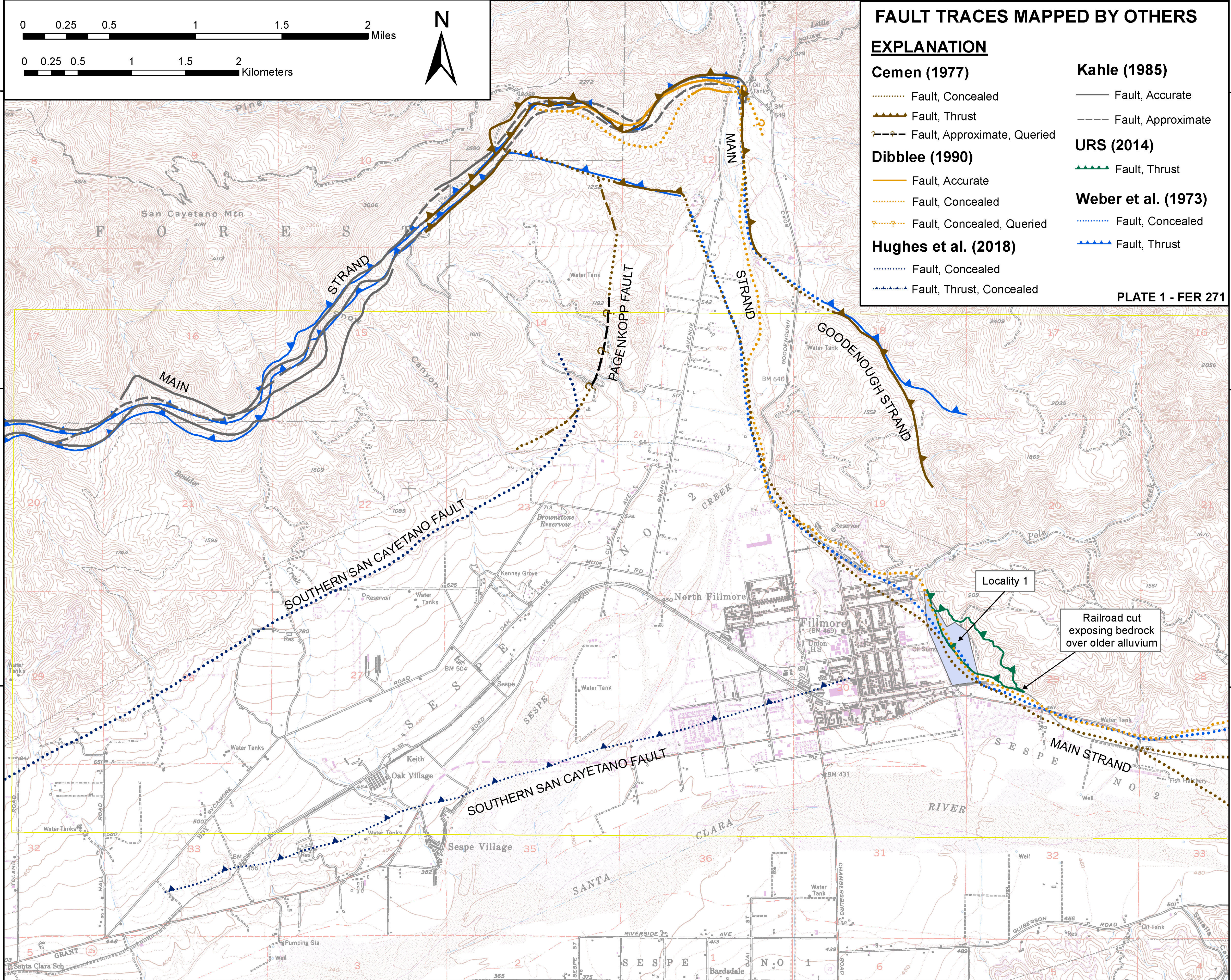


FAULT TRACES MAPPED BY OTHERS

EXPLANATION

- | | |
|------------------------------------|----------------------------|
| Cemen (1977) | Kahle (1985) |
| Fault, Concealed | —— Fault, Accurate |
| ▲▲▲▲ Fault, Thrust | - - - Fault, Approximate |
| ⊕-⊕-⊕- Fault, Approximate, Queried | |
| Dibblee (1990) | URS (2014) |
| —— Fault, Accurate | ▲▲▲▲ Fault, Thrust |
| Fault, Concealed | |
| ⊕-⊕-⊕- Fault, Concealed, Queried | Weber et al. (1973) |
| | Fault, Concealed |
| Hughes et al. (2018) | ▲▲▲▲ Fault, Thrust |
| Fault, Concealed | |
| ▲▲▲▲ Fault, Thrust, Concealed | |

PLATE 1 - FER 271



119°0'0"W 118°58'30"W 118°57'0"W 118°55'30"W 118°54'0"W

34°27'0"N
34°25'30"N
34°24'0"N

34°27'0"N
34°25'30"N
34°24'0"N

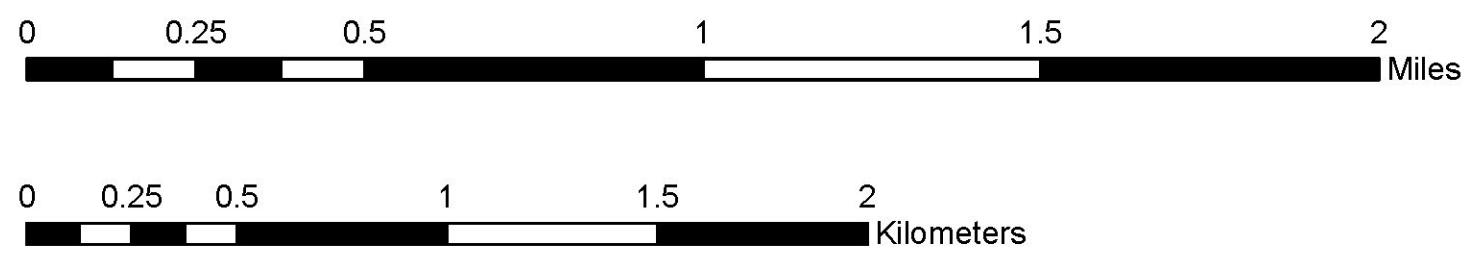
119°0'0"W

118°58'30"W

118°57'0"W

118°55'30"W

118°54'0"W



FAULTS RECOMMENDED FOR ZONING

EXPLANATION

- Fault, Accurate
- - - Fault, Approximate
- Fault, Concealed
- · - · - Fault, Inferred

- Recommended Alquist-Priolo Earthquake Fault Zone
- Existing Alquist-Priolo Earthquake Fault Zones

PLATE 3 - FER 271

QUADRANGLE

PIRU

SANTA PAULA PEAK

QUADRANGLE

34°27'0"N

34°27'0"N

34°25'30"N

34°25'30"N

34°24'0"N

34°24'0"N

119°0'0"W

118°58'30"W

118°57'0"W

118°55'30"W

118°54'0"W

